Fire Hawk Optimized DVR Strategy for Improved Power Quality and LVRT Performance in PV-Connected Grid

D Dinesh
Department of Mechatronics Engineering
Chennai Institute of Technology
Chennai 600069, India
dineshd@citchennai.net

Radhika V
Department of Physics,
Erode Sengunthar Engineering College (Autonomous),
Thudupathy,Perundurai - 638057.
Tamil Nadu, India
radhikaesec@gmail.com

Dr. R. Sundar
Department of Marine Engineering
AMET Deemed to be University
India
Sundar.r@ametuniv.ac.in

Abhinav Pathak
Symbiosis Institute of Computer Studies and Research (SICSR),
Symbiosis International (Deemed University),
Pune, Maharashtra, 411016, India
abhinavgsits7@gmail.com

Debarchita Mishra,
Department of Electrical and Electronics Engineering,
Vels Institute of Science, Technology and Advanced Studies
India
debarchita.se@vistas.ac.in

R. Sreedhar
Department of Electrical and Electronics Engineering
Vel Tech Rangarajan Dr. Sagunthala R&D Institute of Science and Technology
Avadi, Chennai, India.
rsreedhareeeped@gmail.com

2025 8th International Conference on Circuit, Power & Computing Technologies (ICCPCT) | 979-8-3315-4317-4/25/$31.00 ©2025 IEEE | DOI: 10.1109/ICCPCT65132.2025.11176758

***Abstract*— Power Quality (PQ) issues in power distribution networks include voltage sags, swells, and harmonics, all of which disrupt operations. Dynamic Voltage Restorer (DVR) technology is deployed to mitigate these challenges. Existing control methods integrated with DVR systems exhibited drawbacks like steady-state errors, reduced efficiency, and high Total Harmonic Distortion (THD). The introduction of Fire Hawk Optimized (FHO) DVR proven effective in resolving these issues. It uses solar PV cells to power the DVR's DC link, boosted by Interleaved Boost Converter (IBC). It effectively converts low fluctuating PV power into enhanced power for delivering desired power to the DC link. It is managed using Perturb and Observe (P&O) methodology. The efficiency gets further improved the FHO algorithm that produce optimal solution for non-linear optimization problems. Thus, the proposed DVR strategy mitigates PQ issues, minimizes low-order odd harmonic components in the VSI output current and reduces THD. The proposed system's performance tested using Matlab/Simulink. The results validate that enhanced converter efficiency of 95.69% and tracking efficiency of 99.15% is attained, providing a novel method for the enhancement of PV-connected grid performance.**

Keywords—DVR, Fire hawk optimization, Perturb and Observe based MPPT, Interleaved Boost Converter, THD.

I. INTRODUCTION

Electricity quality refers electrical system's ability to provide electricity with pure, noise-free sinusoidal waveform. Enhanced power quality is characterized by stability in both frequency and voltage. However, in real-world scenarios, various loads frequently cause disturbances, leading to deviations from the ideal power supply [1-2]. Power quality challenges encompass harmonics, voltage fluctuations, reactive power compensation, integration constraints, and operational issues. Among these, voltage disturbances pose significant threats to sensitive loads, primarily influenced by the excitation system's time constant and reactive power balance. Numerous approaches have been developed to mitigate the effects of power quality issues [3]

TABLE I. EXISTING WORK.

Ref	Title & Author	Methodology Used	Operations
[4]	Ahmed A. Shehata *et al* [2021] "Efficient Utilization of the Power Grid using FACTS devices based on a new Metaheuristic Optimizer"	Flexible alternating current transmission systems	FACTS boosts the performance of the power systems.
[5]	Abdolmajd Javadian *et al* [2021] "Modeling of static var compensator-high voltage direct current to provide power and improve voltage profile"	Static var compensator and high voltage direct current bonding.	A combination of series and parallel controllers, line impedance management, and voltage regulator successfully regulate system's active and reactive power.
[6]	Sachin Kumar *et al* [2024] " Power quality investigation of a grid-tied hybrid energy system using a D-STATCOM control and grasshopper optimization technique"	Distributed static synchronous compensator	It improves the reliability of electrical system and promotes effective power distribution.

These devices offer quick response times, enabling the injection of reactive power through distribution units. However, despite improvements in power quality, restrictions on active power levels remain necessary [7]. DVR is employed to address voltage-related PQ issues. It injects a voltage with a specific phase angle and magnitude in series with the distribution line to produce a sinusoidal load voltage at the rated level. By mitigating voltage sag and swell problems, the DVR enhances energy utilization efficiency [8].

This paper proposes utilizing a DVR to boost power quality and strengthen the Low Voltage Ride-Through (LVRT) performance of a three-phase medium-voltage network that is integrated into an energy generation system. The DC link gets powered by PV system and the power gets

979-8-3315-4317-4/25/$31.00 ©2025 IEEE

boosted by the DC converter [9]. However, due to external environmental factors like cloud cover, dust buildup, and variations in temperature or sunlight during adverse weather conditions such as rain or snow, the efficiency of PV power generation is significantly affected. These challenges lead to multiple peaks in output power of the PV array, complicating process of tracking the system's maximum power point. Consequently, this results in extended tracking times, decreased efficiency, or errors in tracking, ultimately lowering the overall power generation efficiency. To improve power extraction from PV systems, an improved P&O based MPPT algorithm is employed. Optimization tactics improve the MPPT model's performance.

PSO-based MPPT is a bio-inspired swarm intelligence algorithm where each particle in the swarm represents a possible solution to the optimization problem.

GWO technique mimics the collective behaviour of grey wolves that, tunes the scaling parameters and achieve quick response and reduces steady state error [11].

GWO is a metaheuristic optimization technique that tracks global minim for various nonlinear optimization problems [12].

Nevertheless, these optimization algorithms is sensitive to parameter tuning and get trapped in local optima while handling complex optimization problems. To address, these issues a Fire Hawks optimized algorithm is integrated that exhibit unusual behavior by intentionally spreading fires, carrying burning sticks in their beaks to ignite new areas. The FHO algorithm updates positions by leveraging the superior solutions rather than the global optimum, along with the average of solution candidates. This approach prevents the search process from getting stuck in local optimal points.

Research Gaps:

Despite advances in power quality and LVRT for PV grid integration, there are still limitations to applying complex metaheuristic algorithms such as FHO to optimize DVR strategies. Most research evaluates power quality and LVRT separately, with few combining techniques. Furthermore, there is insufficient validation for a wide range of grid conditions and PV penetration levels, as well as problems with real-time implementation and adaptive control. Addressing these challenges improve the effectiveness and adaptability of DVR systems in PV connected grids.

Contribution of the work:

The proposed model introduces an advanced DVR-optimized control strategy to effectively eliminate power quality issues. It utilizes a solar PV system as the primary energy source for powering the DC link and employs a novel FHO based P&O MPPT controller to ensure maximum power extraction. Additionally, a high-voltage gain is achieved through the implementation of an IBC.

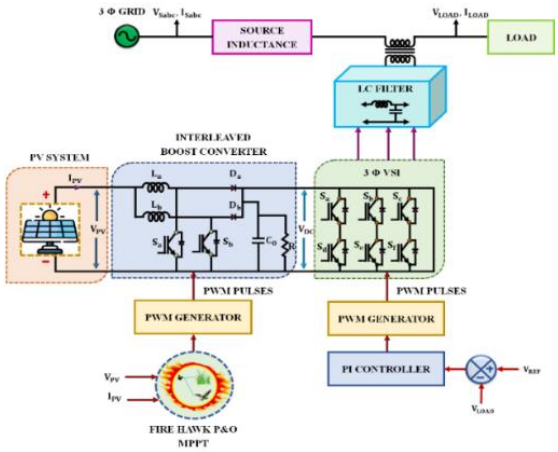

Fig. 1. Block diagram of the proposed model.

The proposed model involves novel approach to enhance PQ, during the energy transfer from source to load. Enhancement of power quality refers to the attributes of current and voltage, including their relationship to frequency variations. Disruptions in power quality adversely affect the distribution network, often resulting in the malfunction or failure of sensitive loads. Key power quality challenges, such as voltage sags, swells, and harmonic disturbances in distribution systems, are efficiently addressed using a DVR paired with advanced intelligent control methods. A block diagram of proposed DVR optimized control strategy is given in fig 1. The PV system provides essential energy to effectively operate the DVR system. The PV system output is fed into the IBC converter and FH optimized P&O based MPPT controller. IBC steps up the voltage levels with high voltage gain and reduced ripple current. The MPPT controller tracks maximum power from the PV system even under dynamic environmental conditions and generates a control signal. The PWM generator produces PWM pulses from the control signal attained by the MPPT controller for enhanced IBC operations. A 3Φ VSI converts the converter's DC voltage to AC power. The PI controller manages 3 VSI operations. It compares reference voltage with actual load voltage and sends control signal to PWM generator. Finally, the optimal power with reduced noise harmonics, is delivered to load.

II. Proposed System Modelling

A. Dynamic Voltage Restorer (DVR)

DVR is connected in series with power distribution system to generate reactive power. It links solar power system on DC side and distribution circuit on AC side. The source current matches load current, but injected voltage remains essentially sinusoidal. The DVR adjusts load voltage during transients, adjusts for harmonics, and maintains a 90° phase shift between (V_f) and (I_s) without using real power. Inverter and filter losses are minimal. The corrected voltage is determined as follows, Kirchhoff's voltage law is applied to phase 1, and the same procedure is followed for the remaining phases.

$$V_s + V_f = I_s(R_s + jX_s) + V_t \quad (1)$$

The source voltage can be expressed as,

$$V_s + V_f = I(Z_s - Z_l) \quad (2)$$

Solving the equation provides (V_f). So, the total DVR voltage required for each phase is:

$$V_{fa} = V_{fa1} + V_{far} \quad (3)$$

$$V_{fb} = V_{fb1} + V_{fbr} \quad (4)$$

$$V_{fc} = V_{fc1} + V_{fcr} \quad (5)$$

$(V_{far}, V_{fbr}, V_{fcr})$ are equal and opposite to the system's harmonics, therefore cancelling it out. To power-up the DC link, energy source is required.

B. PV System

A PV system transforms sunlight into electricity using the photoelectric effect. The PV module's mathematical model is specified using equivalent circuit, which is represented by a single diode with parallel and series resistances, as illustrated in Fig 2.

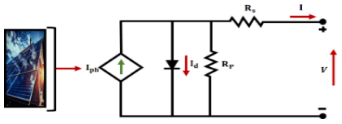

Fig. 2. PV panel circuit

The parameters are determined by well-established method. The current-voltage $(I-V)$ relationship defined as follows,

$$I = I_{ph} - I_0\left[exp\left(\frac{V+IR_S}{aV_t}\right) - 1\right] - \frac{V+IR_S}{R_p} \quad (6)$$

PV panel photocurrent (I_{ph}) is generated by absorbed solar radiation, and (I_0) is diode's reverse saturation current. (R_s) and (R_p) denote panel's series and parallel resistances, respectively. A diode's performance depends on its ideality factor (a), surface temperature (T), and thermal voltage (V_t).

$$I_{ph} = \left(I_{ph,n} + k_i(T - T_n)\right)\frac{G}{G_n} \quad (7)$$

$$I_0 = \frac{I_{ph} - \left(\frac{V_{oc,n}}{R_p}\right)}{exp\left(\frac{V_{oc,n}}{aV_t}\right) - 1} \quad (8)$$

$$V_t = \frac{N_S KT}{q} \quad (9)$$

PV panel performance depends on irradiation level (G), temperature coefficient of short-circuit current (K_i), and standard test condition values $(I_{ph,n})$, $(V_{oc,n})$. It gets influenced by the number of series connected cells, elementary charge, and Boltzmann's constant. Due to the panel's low voltage output, IBC is used to enhance voltage.

C. Interleaved Boost Converter

An IBC consists of parallel connected converters reduce current stress, losses, and output current ripple while improving input current quality. This design increases the converter's rating and overall efficiency. The circuit diagram is shown in Fig. 3.

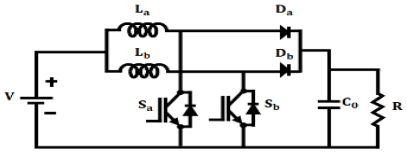

Fig. 3. Interleaved Boost Converter

IBC consists of two parallel switches (S_a, S_b), inductors (L_a, L_b), diodes (D_a, D_b), a capacitor (C), and a load resistor (R), all powered by a reliable input source (V_{in}). The operation is controlled by phase-shifted switching and has four modes, but only the continuous current mode is studied for accessibility. With a temporal delay, inductors and duty cycles are accepted as identical. The mode of operation as shown in Fig 4 and operating waveforms for proposed converter as shown in Fig. 5.

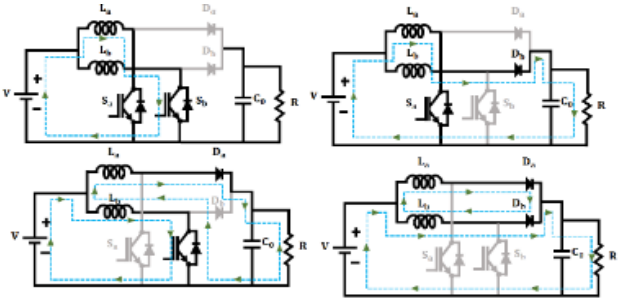

Fig. 4. Operation of mode 1, mode 2, mode 3 and mode 4

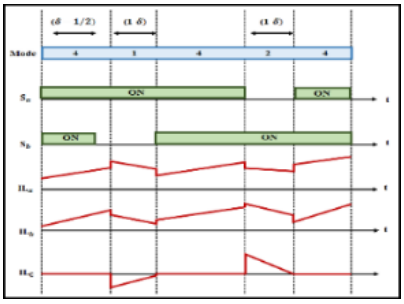

Fig. 5. Operating waveform

Mode 1:

In Mode I, switches (S_a, S_b) are closed, and diodes (D_a, D_b) are reverse biased. The input supply charges the inductors (L_a, L_b), increasing the currents (I_{La}, I_{Lb}).

$$V_{L_a} = V_{in} \quad (10)$$

$$V_{L_b} = V_{in} \quad (11)$$

Mode 2:

In Mode II, switch S_a is closed and S_b is open, turning D_a diode off and D_b on. The input delivers energy to the inductorL_a, which increases the currentI_{La}. Simultaneously, the inductor L_b supplies energy to the load, reducing its currentI_{Lb}.

$$V_{L_a} = V_{in} \quad (12)$$

$$V_{L_b} = V_{in} - V_0 \quad (13)$$

Mode 3:

In Mode III, switch S_a opens and S_b closes, thus diode D_a is forward biased and D_b is reverse biased. Inductor L_a discharges, providing energy to the load but decreasing its currentI_{La}, while the input charges inductorL_b, increasing its currentI_{Lb}.

$$V_{L_a} = V_{in} - V_0 \quad (14)$$

$$V_{L_b} = V_{in} \quad (15)$$

Mode 4:

In Mode IV, switches (S_a, S_b) are open, and the diodes (D_a, D_b) are forward biased, allowing inductors (L_a, L_b) to discharge and power the load. This results in a drop in inductor currents, with the rate of change shown as follows,

$$V_L = V_{in} - V_0 \tag{16}$$

$$\frac{di_{L_a}}{dt} = \frac{di_{L_b}}{dt} = \frac{V_{in} - V_0}{L} \tag{17}$$

For steady-state operations.

$$V_0 = \frac{V_{in}}{(1-\delta)} \tag{18}$$

The minimal inductor values required for continuous conduction mode operation are obtained as follows,

$$L_{a_{min}=L_{b_{min}}} = \frac{V_{in}\delta T}{2\Delta i_L} \tag{19}$$

The minimum inductance values for $(L_a . L_{b_{min}})$ are defined properly. The capacitor (C) is defined as follows,

$$C_{min} = \frac{\delta}{R\left(\frac{\Delta V_0}{V_0}\right) f_s} \tag{20}$$

As discussed in following section, a P&O MPPT controller is used to maintain a constant voltage and ensure FHO operates efficiently.

D. Fire Hawk (FHO) Optimized P&O MPPT Controller

The MPPT integrated within the converter employs P&O technique to optimize duty cycle for optimal PV power. It compares current and previous power values by adjusting the array voltage, which moves the same direction if power increases and reverses if power decreases. While simple and effective, P&O challenges with rapidly changing sun irradiation.

The P&O MPPT technique for its simplicity. In the discrete time domain, it tracks maximum power by measuring the input voltage $V(k)$ and current$I(k)$, then adjusting the duty cycle $D(k)$ accordingly. The duty cycle is updated using Equation (26).

$$D[K] = D[k-1] \pm dD[k] \tag{21}$$

The P&O MPPT controller continuously adjusts the control function to minimize errors. To enhance its performance, this paper introduces the FHO (Forest Hunting Optimization) approach, inspired by the foraging behavior of birds like brown falcons and black vultures, which use fire to flush out prey. As shown in Fig. 6, FHO begins by generating multiple solution candidates to determine the initial positions of forest hunters and prey.

$$X = \begin{bmatrix} X_1 \\ X_2 \\ \vdots \\ X_i \\ \vdots \\ X_N \end{bmatrix} = \begin{bmatrix} x_1^1 & x_1^2 & \cdots & x_1^j & \cdots & x_1^d \\ x_2^1 & x_2^2 & \cdots & x_2^j & \cdots & x_2^d \\ \vdots & \vdots & \vdots & \vdots & \vdots & \vdots \\ x_i^1 & x_i^2 & \cdots & x_i^j & \cdots & x_i^d \\ \vdots & \vdots & \vdots & \vdots & \vdots & \vdots \\ x_N^1 & x_N^2 & \cdots & x_N^j & \cdots & x_N^d \end{bmatrix}, \begin{cases} i = 1,2,\ldots,N \\ j = 1,2,\ldots,d \end{cases} \tag{22}$$

The total distance between the FH and prey is expressed as,

$$D_k^t = \sqrt{(x_2 - x_1)^2 + (y_2 - y_1)^2}, \begin{cases} l = 1,2,..,n. \\ k = 1,2,..,m \end{cases} \tag{23}$$

In this part of the algorithm, a flaming stick is dropped in the designated area to swiftly flush out the prey.

$$FH_1^{new} = FH_1 + (r_1 \times GB - r_2 \times FH_{Near}), \quad l = 1,2,\ldots.,n \tag{24}$$

Prey movements toward FHs and safe zones are guided by r_5 andr_6, with SP_1 and SP defined in equations (33).

$$\left.\begin{aligned} SP_1 &= \frac{\sum_{q=1}^{r} PR_1}{r}, \ \begin{cases} l = 1,2,\ldots,n \\ q = 1,2,\ldots,r \end{cases} \\ SP &= \frac{\sum_{k=1}^{m} PR_1}{m}, \ k = 1,2,\ldots,m \end{aligned}\right\} \tag{25}$$

The FHO optimized DVR strategy improves voltage stability, LVRT performance, and power quality by minimizing sags, lowering harmonics, and enhancing transient responsiveness. It improves DVR performance, reduces power losses, and ensures stable renewable energy integration in modern grids.

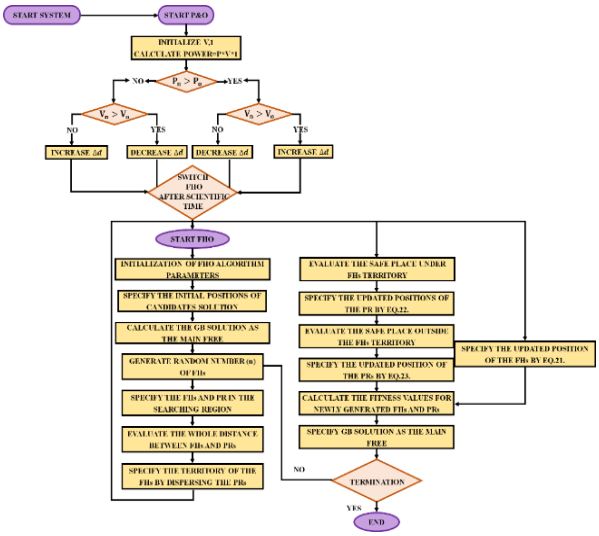

Fig. 6. FHO optimized P&O MPPT controller

III. Results And Discussion

This paper presents the FHO Optimized DVR Strategy, which enhances power quality and LVRT performance in a PV connected grid. The next section discusses the outcomes of proposed work implemented in MATLAB/Simulink 2021a. Parameters and their specifications are shown in TABLE 2.

TABLE II. Parameter Specifications.

Parameter	Specifications
PV System	
Rated Power	$10kW$
No.of panels connected in series	3
No.of panels connected in parallel	16
Open circuit voltage	$37.25V$
Short circuit current	$8.95A$
IBC	
$Inductor\ L_a, L_b$	$22mH$
$Capacitor\ C$	$4.7\mu F$
$Switching\ Frequency$	$10kHz$

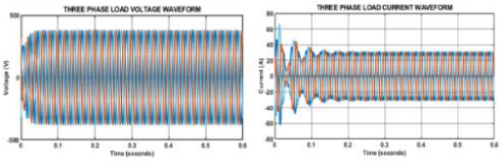

Fig. 7. Waveform of three phase load under sag

Fig. 7 shows the three phase load voltage and current waveforms, with voltage oscillating $\pm 500V$ and current $\pm 60A$. A slight disturbance and transient oscillations appear initially before both stabilize, indicating system stabilization after a switching event and load variation.

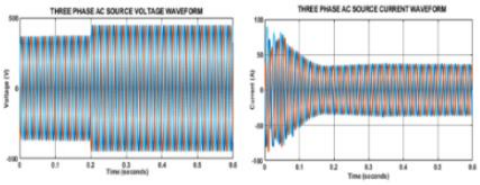

Fig. 8. Waveform of three phase AC source under sag

Fig. 8 represents 3 phase AC Source voltage and current waveforms in case 1, voltage oscillates between $\pm 500V$ and the current between$\pm 100A$. A disturbance around 0.25 seconds disrupts the voltage before stabilizing. The current initially peaks above $100A$, then decrease and settling into a steady oscillatory state beyond 0.3s, indicating system stabilization.

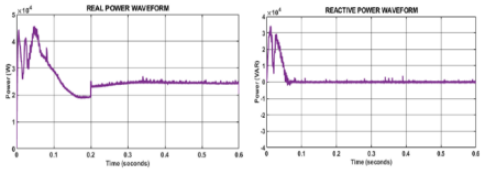

Fig. 9. Real and reactive power waveform

Fig. 9 shows real and reactive power waveforms, initially fluctuating due to a transient response. Real power decrease before stabilizing, while reactive power rises and decrease the system stabilization after load change.

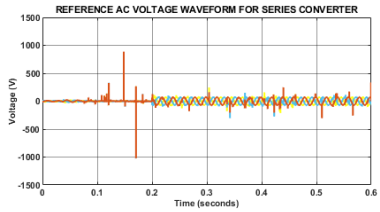

Fig. 10. Waveform of reference AC voltage

Fig. 10 depicts the reference AC voltage waveform for series Converter, which includes severe increases around $\pm 1500V$ due to transient disturbances. After 0.2 seconds, the voltage settles into a consistent oscillating pattern, demonstrating system regulation and steady-state operation.

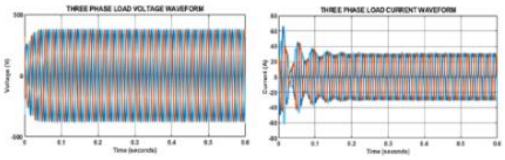

Fig. 11. Waveform of three phase load under swell

Fig. 11 displays the three phase load voltage ±500V and current $\pm 40A$ waveforms. The voltage follows a high-frequency pattern with slight early variations before stabilizing, but the current shows fluctuations, reduced oscillations, and steady-state behavior after 0.2 seconds.

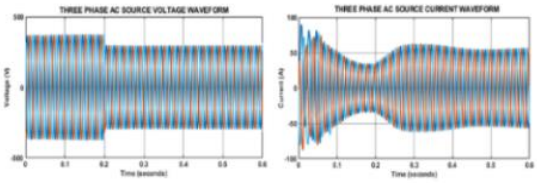

Fig. 12. Waveform of three phase AC source under swell

Fig. 12 displays the three phase AC source voltage $\pm 500V$ and current $\pm 100A$ waveforms. A disturbance at 0.15s induces transitory effects, including voltage oscillations and a current peak of more than 100A. The current slows and stabilizes after 0.3s, indicating a resistive influence.

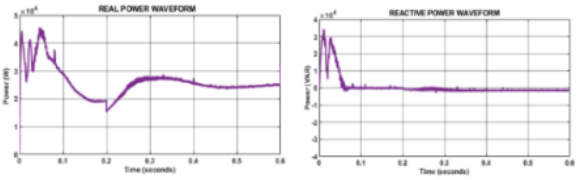

Fig. 13. Waveform of real and reactive power

Fig. 13 shows real and reactive power waveforms. Both exhibit initial fluctuations due to a disturbance, followed by decrease and gradual stabilization beyond 0.3s, indicating system settling after a transient event.

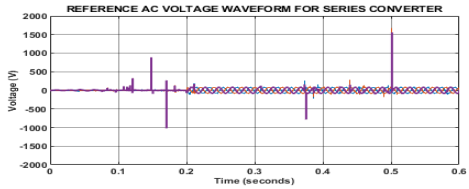

Fig. 14. Reference of AC voltage waveform

Fig. 14 shows the reference AC voltage waveform for a series converter. It oscillates within a nominal range but experiences sharp spikes above $1000V$ and decrease below $-1000V$ around 0.1s and 0.5s, indicating transient disturbances. The waveform then stabilizes into a consistent oscillatory pattern.

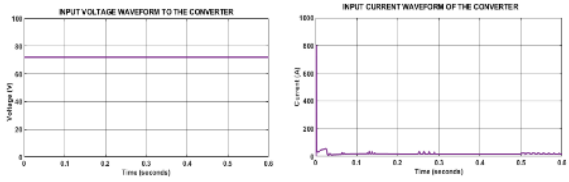

Fig. 15. Converter input waveform.

Fig. 15 presents the input waveform of IBC. The input voltage waveform of the converter it is constantly maintained at $76V$ and current waveform of the converter's input. It is observed that an input current of $22A$ is attained with minimal fluctuations.

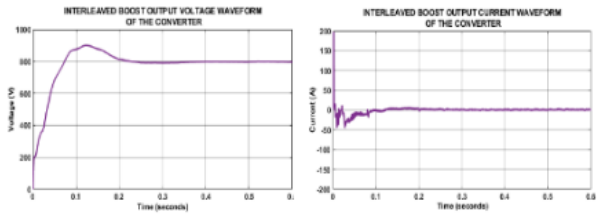

Fig. 16. Converter output waveforms.

Fig. 16 represents the IBC output waveform. The output voltage waveform of the converter after initial peak, voltage is stabilized at$800V$. IBC output current waveform. In initial phase, current is fluctuating after $0.1s$, constant current of $2A$ is obtained.

The THD values for grid system presented in Fig 17, highlighting the variations in harmonic distortion and THD value is 2.98%,

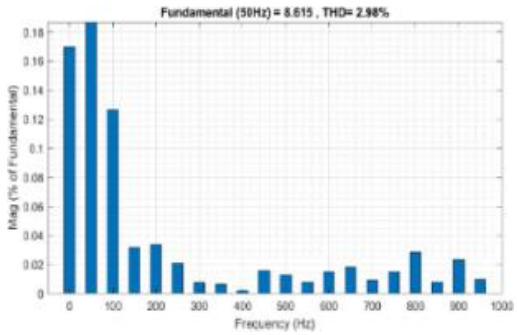

Fig. 17. THD waveform

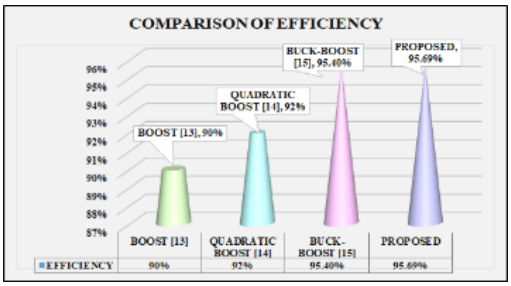

Fig. 18. Comparison of efficiency.

Fig. 18 visualizes the comparison of converter efficiency. It highlights the proposed IBC attains the highest efficiency of 95.69%, while Boost [13] with 90%, Quadratic Boost Converter (QBC) [14] with 92% and buck-boost converter with 95.4%.

TABLE III. TRACKING EFFICIENCY COMPARATIVE ANALYSIS.

Optimized Controllers	Tracking Efficiency
GWO [16]	96.5%
SOA [17]	98.32%
Proposed	99.15%

Table 3 demonstrates the comparative analysis of tracking efficiency with various conventional MPPT optimization algorithms. From the table, the proposed HHO algorithm tracking efficiency is 99.15% which outperforms Grey Wolf Optimization (GWO) [16] algorithm with 96.5% and Seagull Optimization Algorithm (SOA) with 98.32% respectively.

IV. CONCLUSION

In this paper, a new Optimized DVR strategy is developed for enhanced power quality and LVRT performance. The PQ issues related to DC link are addressed by integrating RES based PV system. Power from PV system gets efficiently boosted by the IBC. The proposed converter outperforms standard converters by increasing efficiency and voltage gain. Novel FHO based P&O MPPT approach is implemented and maximum power is extracted from the PV system. Thus, optimal power is delivered from the source to load with enhanced voltage gain. Simulation studies showcase the effectiveness of proposed system. The proposed converter has a greater efficiency of 95.69 % and the algorithm has an efficiency of 99.15%. These findings underscore the viability of the proposed approach in promoting enhanced PQ in grid connected systems.

REFERENCE

[1] P. V. Rathod, *et al* "Performance analysis of a hybrid renewable generation system connected to grid in the presence of DVR," vol. 13, no. 4, pp. 101700, 2022.

[2] N. Visali, "A Short review on Optimal Allocation of Microgrid," Journal of Modern Technology, pp. 132-140, 2024.

[3] S. M. N.Nejrs, *et al* "Innovative control strategies for dynamic load management in smart grid techniques incorporating renewable energy sources," Khwarizmia, no. 2023, pp. 73-83, 2023.

[4] M. J. Alali, "Optimal placement of facts devices to reduce power system losses using evolutionary algorithm," vol. 21, no. 3, pp. 1271-1278, 2021.

[5] T. Sutikno, "Modeling of static var compensator-high voltage direct current to provide power and improve voltage profile," vol. 12, no. 3, pp. 1659-1672, 2021.

[6] R. K. Bindal, "Power quality investigation of a grid tied hybrid energy system using a D-STATCOM control and grasshopper optimization technique," Results in Control and Optimization, no. 14, pp. 100368, 2024.

[7] E. Suriya. "Optimal Integration of Hybrid Energy Sources for Power Flow Management in Grid System," pp. 1-6. IEEE, 2023.

[8] K. E. Okedu, "MPPT for Hybrid Energy System Using Machine Learning Techniques," Journal of Modern Technology, 19-37, 2024.

[9] J. Kim, "Smart Sag Detection and Reactive Current Injection Control for a PV Microgrid under Voltage Faults," Energies, vol. 16, no. 19, pp. 6776, 2023.

[10] K. Al-Haddad, "A PSO-based MPPT algorithm for grid-connected photovoltaic current source inverter," vol. 4, pp. 1-6, 2022.

[11] N. V. Srikanth, "A grey wolf optimized fuzzy logic based MPPT for shaded solar photovoltaic systems in microgrids," vol. 46, no. 18, pp. 10653-10665, 2021.

[12] H. İ. Demir, "A novel modified ant colony optimization based maximum power point tracking controller for photovoltaic systems," vol. 38, pp. 89-93, 2021.

[13] S. Mamun, "An improved non-isolated quadratic DC-DC boost converter with ultra high gain ability," no. 11, pp. 11350-11363, 2023.

[14] M. L. Alghaythi, "Non-isolated high gain quadratic boost converter based on inductor's asymmetric input voltage," no. 9, pp. 162108-162121, 2021.

[15] D. Peftitsis, "An efficient non-inverting buck-boost converter with improved step up/down ability," Energies, vol. 15, no. 13, pp. 4550, 2022.

[16] N. K. Sharma, "Numerical simulation and analysis of grey wolf optimization based maximum power point tracking under complex operational conditions," Acta Energetica, no. 01, pp. 01-13, 2024.

[17] M. Al-Dhaifallah, "A novel MPPT design based on the seagull optimization algorithm for photovoltaic systems operating under partial shading," Scientific Reports, vol. 12, no. 1, pp. 21804, 2022.